

# Carbon Partitioning During Bainite Transformation in 4317 Type Steels

Smati Chupatanakul, Philip Nash\*, and Dajun Chen

Thermal Processing Technology Center  
IIT, 10 W 32<sup>nd</sup> St., Chicago, IL 60616, USA

The carbon partitioning during bainite transformation was studied using a diametrical dilatometer. The relationship of  $M_S$  temperature as a function of carbon content was determined for 4317 type steels. Austempering experiments were performed in which the  $M_S$  temperature was measured as a function of austempering holding time and temperature. The minimum values of carbon content in the residual austenite were determined from measured  $M_S$  temperature values and the relationship to carbon content. The results are compared to the  $T_0$  carbon composition calculated by Thermocalc<sup>TM</sup> for each austempering temperature assuming paraequilibrium. Good agreement is found between the calculated  $T_0$  composition and the final austenite composition.

**Keywords:** 4317 Type Steels, bainite

---

## 1. INTRODUCTION

Bainitic steels are used in a number of applications in industry because bainite structures have good mechanical properties. They are stronger and harder than pearlite and have greater toughness than tempered martensite. The study of bainite transformation kinetics in steels can result in improved mechanical properties over tempered martensite structures [1]. For some components such as gears, a bainitic surface structure with a tempered martensite core provides optimum properties. In order to obtain such a distribution of microstructures, it is necessary for the component to be case carburized. This provides the opportunity to austemper at a temperature which is above the  $M_S$  temperature of the surface region to allow transformation to bainite, but below the  $M_S$  temperature of the core so that a tempered martensite structure is produced. Since case carburization leads to a carbon concentration decreasing away from the surface the bainite transformation kinetics vary with distance. In order to optimize the processing, it is necessary to understand how carbon content affects the bainite transformation kinetics. Bainite transformation kinetics can be determined by dilatometry. Although dilatometry has been used to measure  $M_S$  temperature during bainite transformation [2], the measurements were not made as a function of bainite transformation time and were not correlated to carbon content in the austenite. In this work, we have established the carbon content in austenite as a function of austempering time by

dilatometry.

The carbon concentration of bainitic ferrite during transformation is one of the most important factors to determine and understand the kinetics of carbide precipitation during the bainite transformation. It is widely believed that there is initially a shear transformation of austenite to ferrite of the same carbon content which is followed by the supersaturation of carbon in bainitic ferrite being relieved under paraequilibrium boundary conditions. This occurs by partition into the residual austenite during the bainite transformation and by precipitation of carbon [3-9]. An alternative model has been considered in which the carbon diffuses during the transformation of austenite to bainitic ferrite under equilibrium condition at the interface [3-6]. A third model intermediate between the other two has been considered in which the ferrite grows with a partial supersaturation of carbon and the remaining carbon partitioning into austenite or forming carbides [3-6,8,10-13]. These different models predict different limiting carbon contents in the austenite before the transformation ceases.

## 2. EXPERIMENTAL PROCEDURE

In order to study the carbon partitioning in the carburized case of a 4317 M2 steel, two experimental heats with carbon contents of 0.58 and 0.82 wt.% were produced, Table 1, designated 2358 and 2359. These carbon contents correspond to the mid-point and maximum in the carbon case profile respectively.

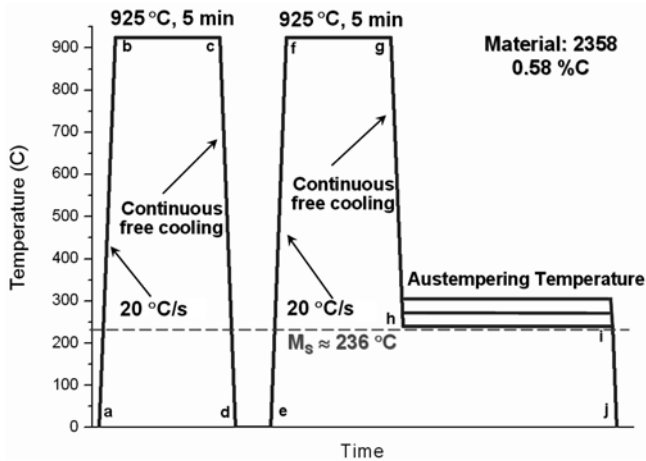
Austempering experiments were performed in order to

---

\*Corresponding author: nash@iit.edu

**Table 1.** Chemical composition of the steels

	C	Mn	P	S	Si	Ni	Cr	Mo	Cu	Sn	Al	V	Nb	Ti
4317 M2	0.18	0.80	0.011	0.022	0.09	1.67	0.56	0.71	0.14	0.007	0.021	0.003	0.014	0.002
2358	0.58	0.82	0.004	0.023	0.04	1.9	0.55	0.77	0.04	-	0.028	-	-	-
2359	0.82	0.86	0.003	0.024	0.04	1.9	0.55	0.76	0.04	-	0.031	-	-	-

**Fig. 1.** Austempering experiment temperature-time profiles for steel 2358.

measure the  $M_S$  temperature change as a function of austempering holding time. The austempering experiments for 2358 were performed in two cycles as shown in Fig. 1. The first cycle is to provide the same microstructure prior to each experiment. The second cycle is the austempering experiment to form bainite above the  $M_S$  temperature. Cylindrical specimens were machined with dimensions 10 mm diameter and 84 mm length and mounted in a Gleeble 3500 thermo-mechanical simulator with a diametrical dilatometer attached to the specimen. The dilatometer was used to measure the diameter change during the thermal processing. After completing the first cycle, the cylindrical specimens were heated to austenitizing temperature (925 °C), held for 5 min and then cooled to different austempering temperatures (i.e. 260, 300, and 340 °C). The specimens were held at the austempering temperature for different times and then cooled to room temperature (25 °C). Longer holding time in the austenite region did not change the  $M_S$  temperature of the steel indicating essentially complete dissolution of carbide.

Optical microscopy and SEM were used to examine the microstructure and analyze the amount of bainite and austenite, after austempering at 260 °C for 17 and 100 min.

### 3. RESULTS AND DISCUSSION

#### 3.1. $M_S$ temperature

As previously reported [14]  $M_S$  temperatures measured for all three materials, which have essentially the same chemical

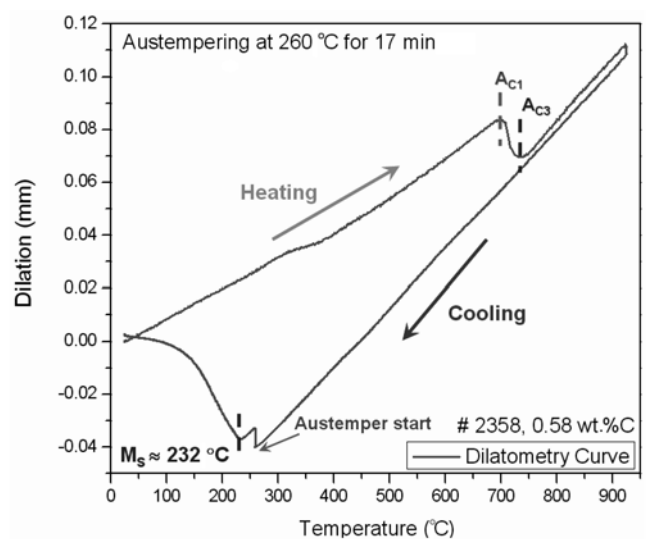
composition except for carbon, were plotted to obtain the relationship of  $M_S$  temperature (°C) as a function of carbon content, and fitting with a polynomial shown in Eq. 1:

$$M_S = 486.4 - 501.9(\text{wt.\%C}) + 122.6(\text{wt.\%C})^2 \quad (1)$$

The  $M_S$  temperature decreases as the carbon content in austenite increases. Using Eq. 1, we can calculate the carbon content for an  $M_S$  temperature corresponding to room temperature (25 °C) which is 1.39 wt.%C and Eq. 1 is assumed to be valid up to this carbon content.

#### 3.2. Carbon content in austenite

From the austempering experiment, the  $M_S$  temperature was measured for each different austempering holding time and temperature during the cooling. As previously reported [14] the  $M_S$  temperature measured for 2358 (0.58 wt.%C) is about 236 °C. Figure 2 shows the dilatometry result for the 0.58 %C alloy austempered at 260 °C for 17 min, where it can be seen that the  $M_S$  temperature decreased from 236 to 232 °C. Prior to the austempering there are no other transformations during cooling, confirming that the cooling rate is sufficient to avoid the pearlite nose of the C curve of the TTT diagram. There is a decrease of the  $M_S$  temperature upon austempering the material as a function of time for

**Fig. 2.**  $M_S$  temperature measurement using dilatometry curve after austempering at 260 °C for 17 min.

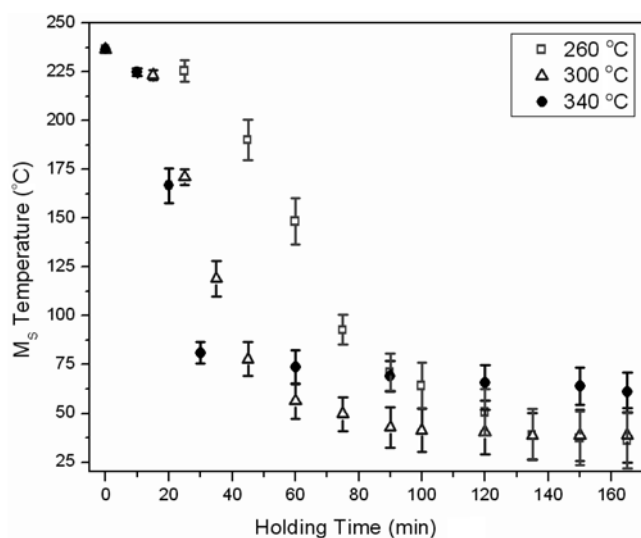


Fig. 3.  $M_s$  temperature as a function of austempering holding time.

each austempering temperature. This decrease of  $M_s$  temperature is due to the rejection of carbon from bainite into austenite. Figure 3 shows the results of  $M_s$  temperature as a function of holding time for austempering temperatures of 260, 300, and 340 °C. Each data point represents the average of at least 3 measurements.

Austenite carbon content was calculated by taking the  $M_s$  temperature data as a function of austempering time and using Eq. 1. Figure 4 shows the relationship of the carbon content in austenite as a function of holding time. Upon austempering at 260, 300, and 340 °C, there is an increase in

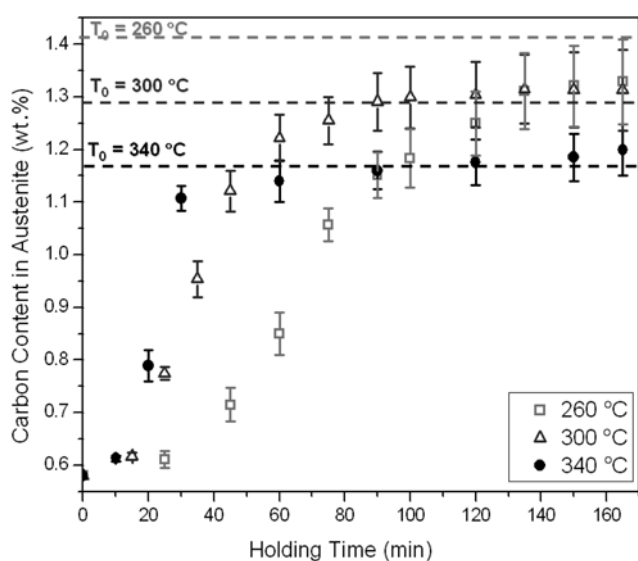


Fig. 4. Carbon content in austenite as a function of austempering holding time with calculated  $T_0$  composition at each austempering temperature.

carbon content in the austenite due to rejection of carbon from the bainite. However, the austenite carbon content reaches a limiting value, depending upon the austempering temperature, of about 1.32 and 1.2 wt.%C for 300 and 340 °C respectively. Measurement of  $M_s$  temperature below room temperature (25 °C) is currently not possible with the experimental set up and so the limiting value for austenite carbon content for austempering at 260 °C cannot currently be measured. For austempering at 260 °C, the maximum value of austenite carbon content measured is about 1.34 wt.%C as shown in Fig. 4 but the curve is clearly still rising with austempering time. As expected, the carbon rejection rate is higher at higher austempering temperatures.

In this work, the calculation of carbon content in austenite assumes paraequilibrium i.e. only carbon is partitioned during the bainite transformation. If other elements partition, they will alter the  $M_s$  temperature. The chemical composition of austenite was predicted by assuming that the bainite grows without any initial diffusion, and then some of the excess carbon is partitioned into the residual austenite and some as carbide precipitates.

The transformation from austenite to bainite of the same composition has a thermodynamic driving force as long as the austenite has a higher free energy than the ferrite [3,5,6]. Ignoring any strain energy associated with the growth of bainite, the carbon content corresponding to  $T_0$  at the austempering temperature,  $T_A$ , will define the limit for the bainite transformation.  $T_0$  is the temperature at which austenite and ferrite of identical composition have equal Gibbs free energy and there is zero driving force. Once the austenite carbon concentration has reached that corresponding to the  $T_0$  for that particular austempering temperature the transformation ceases. The bainite transformation cannot proceed if the carbon content of the austenite is beyond that corresponding to  $T_0$  [3,5,6,15,16]. This reaction is said to be incomplete, since the austenite has not achieved its equilibrium composition (given by the  $Ae_3$  curve) at the point the reaction stops [3,5,6,17,18].

In order to ascertain if the limiting carbon content measured experimentally corresponds to the composition at  $T_0$ , free energy curves for ferrite and austenite in 2358 were calculated as a function of carbon content using ThermoCalc™, Fig. 5, upper graph. The  $T_0$  calculation plot is shown in Fig. 5, lower graph, and a linear fit to the data gives:

$$T_0 = 733.2 - 33609W(C) \quad (2)$$

The carbon composition for  $T_0$  is given in weight fraction of carbon ( $W(C)$ ). From the above equation the carbon compositions corresponding to  $T_0$  of 260, 300, and 340 °C, are 1.41, 1.29, and 1.17 wt.%C respectively. The limiting carbon contents corresponding to  $T_A = T_0$  are compared with the experimental results in Fig. 4. For austempering at 300 and

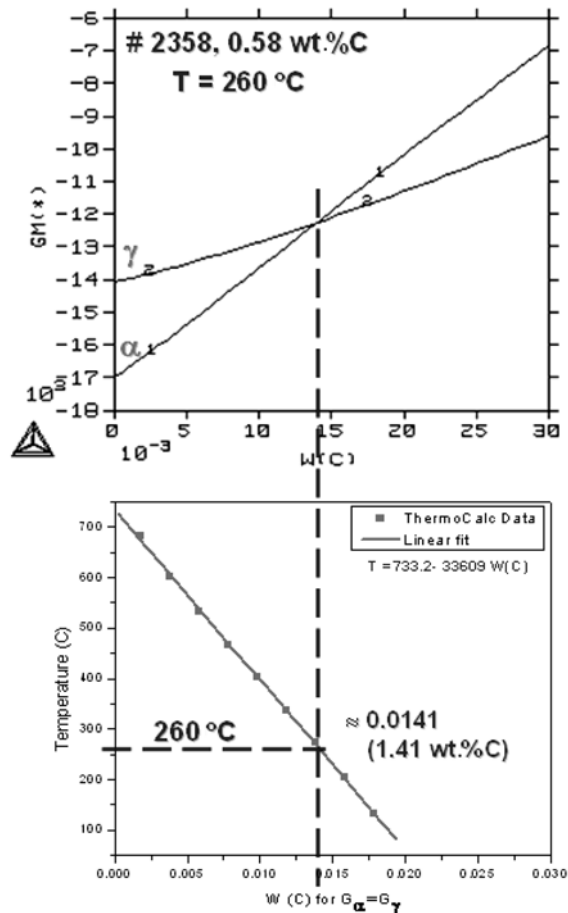


Fig. 5. Calculated free energy curves for ferrite and austenite (upper graph) and  $T_0$  curve (lower graph) for 2358 at 260 °C.

340 °C, it is clear that there is excellent agreement between the measured limiting austenite carbon content achieved during the bainite transformation and the calculated carbon content corresponding to  $T_0$ . For austempering at 260 °C, there is a limitation of the  $M_S$  temperature measurement because  $M_S$  temperature for an austempering time exceeding 180 min is lower than room temperature (25 °C), and so the carbon content in the austenite due to rejection of carbon from the bainite could not be measured experimentally at the limiting value from calculation of  $T_0$ .

### 3.3. Microstructure analysis

The microstructure at an early stage of the bainite transformation in 2358 (0.58 wt.%C), which was austempered at 260 °C for 17 min, is shown in Fig. 6. In Fig. 6(a) with lower magnification ( $\times 400$ ), it shows a small amount of lower bainite (dark) and a large amount of martensite combined with a small amount of retained austenite (light) as expected from the results from the dilatometry curve shown in Fig. 2. From Fig. 6(b) with higher magnification ( $\times 1,000$ ), it was

found that each single bainitic ferrite plate consists of many parallel thin bainitic ferrite platelets, which is verified by the SEM micrograph (Figs. 6(c) and (d)) at the early stage of the formation of bainite. This suggests that the bainitic ferrite will start to form as parallel thin platelets with the carbides precipitating in one variant of the orientation relationship. Then they will grow in both longitudinal and lateral directions and meet together side by side to form the larger bainitic ferrite plate as shown in the optical micrograph (Fig. 6(b)). The details of this suggested new mechanism for the bainite transformation will be discussed in a separate paper.

The microstructure of the lower bainite after austempering at 260 °C for 100 min is shown in Fig. 7. It shows that with elongated holding time, the microstructure (Fig. 7(a)) is mostly lower bainite, with a small amount of martensite and retained austenite. The SEM micrograph (Fig. 7(c)) shows very clearly that in some areas, the carbides not only precipitate inside but they also precipitate between the bainitic ferrite platelets. This is different from the typical morphology of lower bainite [7,11,19-21], in which the carbides mainly precipitate within the bainite and frequently precipitates in just one variant of the orientation relationship forming parallel arrays at about 60° with the long axis of the bainitic ferrite plate, as shown in Fig. 7(b). Bhadeshia [22] found that holding at temperature after the bainite transformation in Fe-0.3C-4.08Cr wt.% is completed causes precipitation of carbides between the bainitic ferrite platelets due to the diffusional (reconstructive) decomposition of the carbon enriched austenite.

## 4. CONCLUSIONS

The carbon content in residual austenite during the transformation to bainite at constant temperature was determined as a function of time by using the relationship between  $M_S$  temperature and carbon content as shown in Eq. 1. During the bainite transformation, the carbon content in the residual austenite increases with increase of austempering holding time. The carbon content in austenite determined from the measured  $M_S$  temperature represents the minimum carbon content in the residual austenite. The maximum values of carbon content obtained in the residual austenite from our experiments (austempering at 300 and 360 °C) show excellent agreement with the values of carbon content corresponding to  $T_A = T_0$  calculated from ThermoCalc%. There is a practical limitation on the  $M_S$  measurement, since  $M_S$  temperatures below room temperature (25 °C) cannot currently be measured with our experimental set up. These experimental results directly support the model of formation of fully supersaturated bainitic ferrite with the same composition as the austenite from which it forms, followed by partitioning of carbon from ferrite to austenite. The transformation ceases after the carbon content in the austenite reaches the  $T_0$  com-

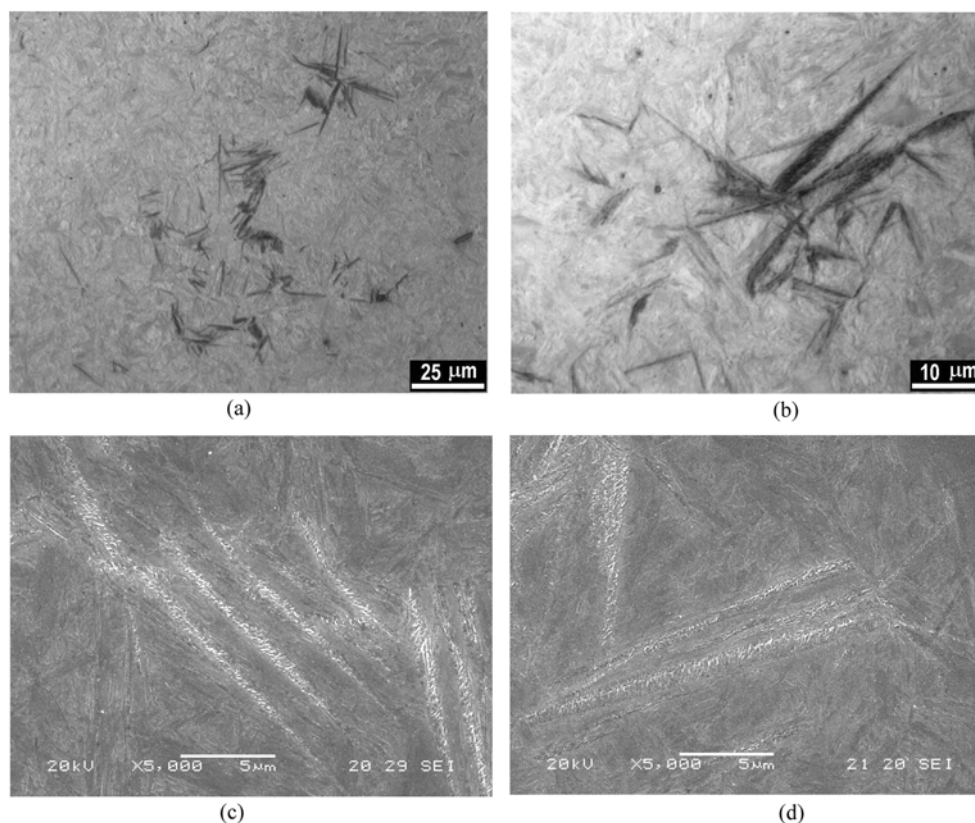


**Fig. 6.** Microstructure analysis of 2358 austempering at 260 °C for 17 min: (a) at  $\times 400$  and (b) at  $\times 1000$  optical micrograph; (c) and (d) SEM micrograph.

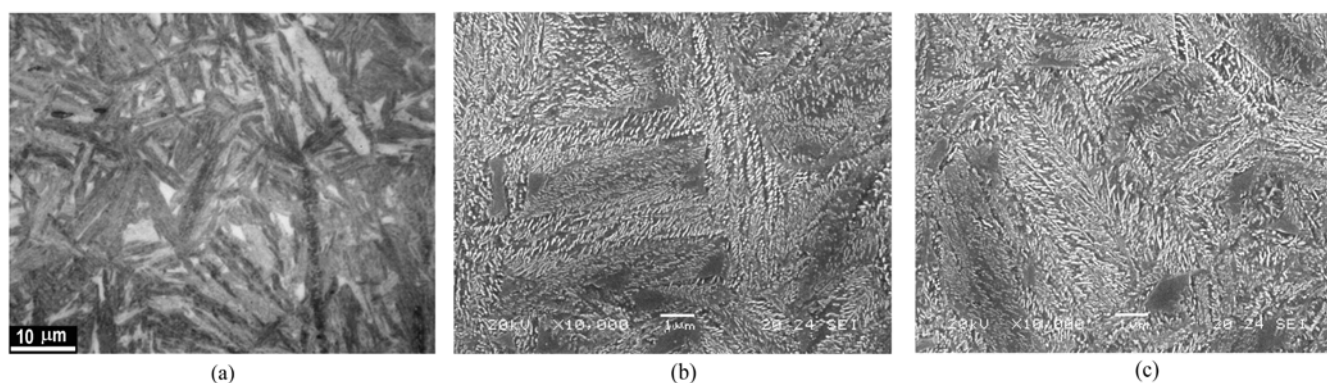


**Fig. 7.** Microstructure analysis of 2358 austempering at 260 °C for 100 min: (a) at  $\times 1000$  optical micrograph; (b) and (c) SEM micrograph.

position at the austempering temperature. The microstructure observed is typical lower bainite, the carbide precipitates within the bainite and precipitates in just one variant of the orientation relationship and forms parallel arrays at about  $60^\circ$  with the long axis of the bainite plate.

#### ACKNOWLEDGEMENTS

The authors wish to thank Mr. R. Binoniemi of Dana Corporation for helpful discussions, provision of material and

financial support of this project. The first author is also grateful to the TPTC at IIT for the provision of a Finkl Fellowship.

#### REFERENCES

1. C. Garcia-Mateo, F. G. Caballero, and H. K. D. H. Bhadeshia, *Mat. Sci. Forum* **500-501**, 495-502 (2005).
2. Z. Lawryniewicz, *Mat. Sci. and Tech.* **18**, 1322 (2002).
3. H. K. D. H. Bhadeshia, *Bainite in Steels*, Institute of Mate-

- rials, London, U.K. (2001).
4. J. G. Speer, D. V. Edmonds, F. C. Rizzo, and D. K. Matlock, *Solid State & Mat. Sci.* **8**, 219-237 (2004).
  5. H. K. D. H. Bhadeshia and J. W. Christian, *Metall. Trans. A* **21**, 767-797 (1990).
  6. R. W. K. Honeycombe and H. K. D. H. Bhadeshia, Edward Arnold, London, 2<sup>nd</sup> edition (1995).
  7. S. Mujahid and H. K. D. H. Bhadeshia, *Acta metall. mater.* **41**, 389-396 (1992).
  8. M. Hillert, L. Hoglund, and J. Agren, *Acta metal. mater.* **41**, 1951-1957 (1993).
  9. D. Van Dooren, B. C. De Cooman, and P. Thibaux, *Proceedings of the International Conference on Advanced High Strength Sheet Steels for Automotive Application*, p. 247-257, Warrendale, PA: AIST (2004).
  10. J. Agren, *Acta metall.* **37**, 181-189 (1989).
  11. G. B. Olson, H. K. D. H. Bhadeshia, and M. Cohen, *Acta metall.* **37**, 381-389 (1989).
  12. G. B. Olson, H. K. D. H. Bhadeshia, and M. Cohen, *Metal Trans. A* **21**, 805-809 (1990).
  13. S. A. Mujahid and H. K. D. H. Bhadeshia, *Acta metall. mater.* **41**, 967-973 (1993).
  14. S. Chupatanakul and P. Nash, *J. Mater. Sci. Lett.* **41**, 4965-4969 (2006).
  15. J. W. Christian and D. V. Edmonds, *Phase Transformations in Ferrous Alloys* (eds, A. R. Marder and J. I. Goldstein), p. 293-326, TMS-AIME, Warrendale, PA (1984).
  16. G. I. Rees and H. K. D. H. Bhadeshia, *Mater. Sci. Tech.* **8**, 985-993 (1992).
  17. D. J. Hall, H. K. D. H. Bhadeshia, and W. M. Stobbs, *Journal de Physique, Colloque C4* **43**, 449-454 (1982).
  18. H. K. D. H. Bhadeshia, *Proc. Int. Solid-Solid Phase Transform. Conf.*, p. 1041-1048, Pittsburgh (1981).
  19. P. G. Shewmon, *Transformation in Metals*, p. 238, McGraw-Hill, New York (1969).
  20. R. F. Hehemann, *Ferrous and Non-Ferrous Bainitic Structures, Metallography, Structure, and Phase Diagrams, 8<sup>th</sup> ed.*, American Society for Metals (1973).
  21. ASM Handbook, *Metallography and Microstructures*, Vol. 9, ASM International, Materials park, OH, USA (2004).
  22. H. K. D. H. Bhadeshia, *Acta metall.* **28**, 1103-1114 (1979).